Research Square

Preprints are preliminary reports that have not undergone peer review.
They should not be considered conclusive, used to inform clinical practice,
or referenced by the media as validated information.

Qualitative CT Features as Predictors of Microscopic Perinephric Fat Invasion in Renal Cell Carcinoma: Towards a Radiomics-Informed Staging Framework

Wei Zheng So

soweizhengs@gmail.com

National University Health System

Kaiying Wang

National University Health System

Ziting Wang

National University Health System

Han Yang Ong

National University Health System

Jonathan Sng

National University Health System

Eric Fang

National University Health System

Edmund Chiong

National University Health System

Ho Yee Tiong

National University of Singapore

Research Article

Keywords: Carcinoma, Renal Cell, Neoplasm Staging, Nephrectomy, Nomograms, Tomography, X-Ray Computed

Posted Date: November 11th, 2026

DOI: https://doi.org/10.21203/rs.3.rs-11331355/v1

License: This work is licensed under a Creative Commons Attribution 4.0 International License.
Read Full License

Additional Declarations: No competing interests reported.

Qualitative CT Features as Predictors of Microscopic Perinephric Fat Invasion in Renal Cell Carcinoma: Towards a Radiomics-Informed Staging Framework

Abstract

Purpose Up to 14% of cT1 renal cell carcinomas (RCC) treated with partial nephrectomy are upstaged to pT3a owing to microscopic perinephric fat invasion (PFI) not visible on preoperative computed tomography (CT). We aimed to identify reproducible qualitative CT predictors of microscopic PFI.

Methods Consecutive patients undergoing partial nephrectomy for cT1 RCC without overt local invasion (2009–2020) were enrolled in a prospective database. Pre-specified CT features were scored by a blinded primary radiologist and re-scored by two further blinded readers. Associations with PFI were modelled using Firth penalised logistic regression and inter-reader agreement with Fleiss' κ. A two-feature nomogram was internally validated by bootstrap.

Results Of 135 patients, 117 formed the imaging cohort; 10 (8.5%) had PFI. Tumour margin irregularity (odds ratio [OR] 5.20, 95% confidence interval [CI] 1.45–22.6) and perinephric neovascularity (OR 4.84, 95% CI 1.31–18.0) predicted PFI on univariable analysis, whereas fat stranding did not (OR 0.95). Three-reader agreement was substantial (κ 0.67–0.74). After mutual adjustment, neither feature remained significant (margin irregularity OR 3.56, 95% CI 0.78–17.8; neovascularity OR 2.41, 95% CI 0.55–10.9). The nomogram achieved an optimism-corrected area under the curve of 0.71 (apparent 0.73, 95% CI 0.54–0.90).

Conclusion Margin irregularity and neovascularity are candidate CT predictors of microscopic PFI in cT1 RCC, whereas peritumoural fat stranding is not. Tumour margin irregularity, the strongest univariable predictor with substantial inter-reader agreement, is a practical marker to report when staging cT1 RCC and a biologically anchored target for future radiomics models, pending external validation.

Keywords Carcinoma, Renal Cell; Neoplasm Staging; Nephrectomy; Nomograms; Tomography, X-Ray Computed

Introduction

Renal cell carcinoma (RCC) is among the ten most frequently diagnosed cancers [1], accounting for 2% of all malignancies globally [2]. The majority of patients are diagnosed incidentally on imaging, with more than two-thirds clinically staged as T1 [3]. The treatment of choice for T1 RCC is partial nephrectomy (PN) for renal function preservation [4]. Preoperative staging of RCC is routinely performed with computed tomography (CT), which can detect overt signs of local invasion with a reported sensitivity of up to 88% [5]. However, despite best efforts, up to 14% of patients are postoperatively upstaged to pT3a [6,7] owing to microscopic perinephric or renal sinus fat invasion not visible on preoperative imaging. These patients have worse outcomes, with higher rates of positive surgical margins [8], higher recurrence, and reduced cancer-specific survival [9]. Treatment considerations may also differ, as some studies report that radical nephrectomy in patients upstaged to pT3a is associated with lower recurrence than PN [10].

While extensive literature exists on the utility of CT in identifying overt local invasion, a remaining gap is the inability to predict which patients with no invasion on imaging will be upstaged after histopathological examination.

This gap has prompted growing interest in structured imaging classification systems for renal masses. The American College of Radiology has recently adopted a Kidney Imaging Reporting and Data System (KI-RADS) as a work-in-progress framework, with the explicit objective of predicting not only the likelihood of cancer but the likelihood of aggressive biological behaviour [11]. Analogous to BI-RADS and PI-RADS, KI-RADS will require a robust evidence base identifying which imaging features carry prognostic signal. In parallel, radiomics, the high-throughput extraction of quantitative imaging features, has shown early promise for predicting pT3a upstaging and perinephric fat invasion (PFI) in RCC [12,13], but

the biological relevance of radiomic features is maximised when they are anchored to anatomically and pathologically meaningful regions of interest.

This study aimed to identify qualitative CT features that predict microscopic PFI in patients with cT1 RCC undergoing PN. By characterising these features in a prospective, pathologically validated cohort, we sought to establish a biologically grounded foundation for future quantitative radiomics models and for KI-RADS feature selection.

Methods

Patient selection, imaging and histological interpretation

All consecutive patients who underwent PN for solid renal tumours at our institution between December 2009 and March 2020 were recruited into a prospective observational database, with clinical, operative and pathological data recorded at the time of surgery. Inclusion criteria were: (a) pathologically confirmed RCC, (b) staged preoperatively as T1 on contrast-enhanced CT with no overt signs of local invasion, and (c) PN with curative intent. Patients were excluded if they had undergone renal tumour biopsy before surgery, or if final pathology revealed a diagnosis other than RCC.

All preoperative CT scans were reviewed by an independent radiologist specialising in urological imaging (primary reader), blinded to patient identities, clinical histories, and pathological outcomes. These scores were used for all association and modelling analyses. To assess reproducibility of the qualitative features, all scans were independently re-scored by two additional blinded radiologists using the same written definitions. The following tumour characteristics were collected: tumour margin irregularity (a non-smooth, lobulated tumour outline relative to the adjacent or contralateral normal renal contour), neovascularity (irregular small vessels within perinephric fat), fat stranding (change in attenuation of peritumoural fat), tumour location (contact with cortex) and enhancing nodules in the perinephric space.

These features were selected a priori for biological plausibility and prior qualitative CT evidence, and represent the tumour–fat interface zones identified as priority regions of interest for peritumoural radiomics in RCC [14].

Statistical analysis

All statistical analyses were performed in R version 4.4.1 (R Foundation for Statistical Computing, Vienna, Austria). Patients with and without PFI were compared using the chi-squared or Fisher's exact test for categorical variables and the independent t-test for continuous variables. Inter-observer agreement across the three readers was quantified using Fleiss' κ with bootstrap 95% confidence intervals (CI), with pairwise Cohen's κ also reported; agreement was interpreted per Landis and Koch (0.61–0.80 substantial, >0.80 almost perfect). Diagnostic performance of each feature (sensitivity, specificity, positive and negative predictive values [PPV, NPV]) was calculated against the histological reference standard using the primary reader's scores. Given the low number of events, associations with PFI were modelled using Firth penalised logistic regression, which reduces the small-sample bias of ordinary maximum-likelihood estimation and yields finite estimates under quasi-complete separation. Odds ratios (OR) are reported with profile penalised-likelihood 95% CI, and covariate significance was assessed by penalised likelihood-ratio tests in univariable and multivariable models. Features associated with PFI on univariable analysis and present in sufficient numbers to avoid quasi-complete separation were entered into a multivariable model (margin irregularity and neovascularity). Fat stranding, which was pre-specified but showed no univariable association, was not carried forward. The multivariable model was converted to a nomogram. Discrimination was summarised by the area under the receiver-operating-characteristic curve (AUC; pROC package) with a percentile bootstrap 95% CI. Internal validation used bootstrap optimism correction (rms package) to derive an optimism-corrected AUC and calibration slope. Given ten events, the nomogram is presented

as exploratory and hypothesis-generating. A two-sided $p<0.05$ was considered statistically significant.

Results

Baseline characteristics

Of 135 patients, 117 formed the imaging-analysis cohort; 18 were excluded because preoperative CT images were not accessible for review. The imaging-analysis cohort was comparable with the full surgical series in age (mean 58.9 vs. 58.2 y), male sex (71.8% vs. 71.1%), body mass index (26.7 vs. 26.5 kg/m²) and clear-cell histology (81.2% vs. 80.7%). On postoperative histology, 10 patients (8.5%) in the imaging-analysis cohort had PFI. Age, CT tumour size and RENAL nephrometry components did not differ significantly between patients with and without PFI (Table 1).

Predictive factors for perinephric fat invasion

Tumour margin irregularity and neovascularity were more frequent in tumours with PFI (Table 2) and were significant univariable predictors of PFI (Table 3). Fat stranding was not significant. An enhancing nodule in the perinephric space was also associated with PFI but was present in only four patients (two with PFI) and was therefore not carried into multivariable modelling to avoid quasi-complete separation.

On Firth penalised multivariable logistic regression including margin irregularity and neovascularity, both features were associated with increased odds of PFI, although neither reached statistical significance after mutual adjustment (margin irregularity OR 3.56, 95% CI 0.78–17.8, p=0.10; neovascularity OR 2.41, 95% CI 0.55–10.9, p=0.24) (Table 3, Fig. 1). The two features overlapped substantially—13 of the 18 tumours with neovascularity also had irregular margins—so their independent contributions could not be separated at this event count. The multivariable model discriminated PFI with an apparent AUC of 0.73 (bootstrap

95% CI 0.54–0.90) and an optimism-corrected AUC of 0.71 (calibration slope 0.98); margin irregularity alone achieved an AUC of 0.71 (95% CI 0.53–0.86) (Fig. 2).

The two-variable model was converted into a nomogram (Fig. 3). Observed and predicted PFI rates for the four possible feature combinations are shown in Table 5. Tumours with neither feature (63%) had an observed PFI rate of 4%, whereas tumours with both features had a rate of 28%.

Inter-observer agreement and diagnostic performance

Agreement across the three readers was substantial for tumour margin irregularity (Fleiss' κ=0.67, 95% CI 0.55–0.77), neovascularity (κ=0.74), perinephric fat stranding (κ=0.68) and enhancing nodule (κ=0.65), and almost perfect for contour abutment (κ=0.83) (Table 4, Fig. 4). Pairwise agreement between the two reproducibility readers was 0.79 (95% CI 0.67–0.90) for margin irregularity, exceeding the moderate agreement (κ=0.50) previously reported for tumour-edge assessment [5]. Margin irregularity had a sensitivity of 0.70, specificity of 0.71, PPV of 0.18 and NPV of 0.96 for PFI (Table 4).

Predictive factors for pT3a upstaging

Eleven patients (9.4%) were upstaged to pT3a: ten with PFI (one with concurrent renal sinus fat invasion [RSI]) and one with RSI alone. On univariable Firth regression, tumour margin irregularity (OR 3.99, 95% CI 1.18–15.0, p=0.026), neovascularity (OR 4.05, 95% CI 1.13–14.2, p=0.033) and an enhancing perinephric nodule (OR 11.0, 95% CI 1.54–79.4, p=0.019) were associated with pT3a upstaging, whereas fat stranding was not (OR 1.14, 95% CI 0.34–3.94, p=0.83).

Discussion

While much is known about CT detection of macroscopic invasion, microscopic PFI and RSI remain difficult to predict. Sokhi et al. [5] found microscopic invasion was the sole evidence of T3a stage in 45% of pT3a patients, yet readers predicted microscopic RSI in only

35.7%–42.9%. Prior attempts to use secondary CT factors have been inconclusive [15], partly owing to varying inclusion criteria. By including only patients with no overt invasion who underwent PN, our study more directly evaluates CT factors predictive of upstaging due to PFI and RSI.

Radiomics offers reproducible, objective characterisation of the tumour–perinephric fat interface, and preliminary PFI radiomics models show accuracy exceeding individual radiologists [12]. However, data-driven radiomics risks identifying statistically associated but biologically arbitrary features; our prospective, pre-specified design provides a biologically informed target space, the tumour margin zone and peritumoural fat, for radiomic feature engineering.

Contour irregularity has previously been linked to RSI [16,17], with conflicting evidence [18] attributed to reader subjectivity; inter-rater agreement on tumour edge was only moderate (κ=0.50) in one study [5]. In our cohort, by contrast, agreement on margin irregularity was substantial (Fleiss' κ=0.67 across three readers; 0.79 between the two reproducibility readers), supporting its clinical usability and its suitability as an anchor for shape-based radiomic descriptors.

Quantitative shape descriptors (sphericity, surface-to-volume ratio, fractal dimension) are mathematical operationalisations of this phenotype. Consistent with our findings, Shimada et al. showed that radiomics based on dynamic CT, with tumour shape irregularity as the key feature, predicted pT3a upstaging in cT1b–2 RCC [19]. More recently, Lee et al. identified irregular margins (OR 3.40) and lobulated shape as independent CT predictors of PFI in a size-matched case–control nephrectomy series, with increased perirenal vascularity also more prevalent among tumours with PFI [20]; our findings extend this observation to cT1 tumours without overt invasion selected for PN. That margin irregularity was the strongest and most reproducible predictor in our cohort, with neovascularity a correlated marker of the same

tumour–fat interface phenotype, reinforces this convergence between qualitative observer assessment and quantitative radiomics. Clinically, when margin irregularity is identified, consideration might be given to adjusting the plane of resection to preserve a cuff of perinephric fat rather than dissecting along the pseudocapsule, although the modest PPV of the feature (0.18) means that most such tumours will not harbour PFI; its high NPV (0.96) may be the more actionable property.

Fat stranding warrants discussion. While some studies find it predictive of PFI or higher pathological T stage [21-23], concerns about low specificity exist [24]; it is a non-specific sign with many causes [25] and becomes increasingly so as tumour size increases [18]. We found fat stranding was not predictive, having restricted scoring to peritumoural rather than generalised stranding to mitigate its low specificity. Cohorts in which stranding is predictive have typically included larger or overtly invasive tumours, whereas our cohort was restricted to cT1 tumours without overt invasion. From a radiomics perspective, the relevant signal may lie in peritumoural fat at defined radial distances rather than in global perirenal fat, consistent with emerging clear-cell RCC data [14].

Limitations include the small number of events, which precluded correlation with long-term oncological outcomes, and the differing prognosis RSI may confer relative to PFI [26]. The nomogram is derived from ten events and is presented as exploratory; margin irregularity and neovascularity are correlated, their independent contributions cannot be separated in this cohort, and external validation is required before any clinical use. The qualitative nature of feature assessment is a further limitation, although our substantial inter-observer agreement partially mitigates this; future studies should incorporate semi-automated quantitative measurement to enable robust model training. To our knowledge this is the first study to examine blinded, multi-reader qualitative CT features as predictors of microscopic PFI specifically in patients undergoing PN. Our identification of margin irregularity and

neovascularity as candidate predictors, and of peritumoural fat stranding as non-contributory, provides a biologically grounded framework for prospective radiomics model development; larger multicentre cohorts will be required to train and validate such models and to explore their integration within a KI-RADS-aligned reporting framework. In summary, tumour margin irregularity is a reproducible qualitative CT marker of occult perinephric fat invasion in cT1 RCC that merits prioritisation in structured reporting and in radiomics feature engineering.

Conclusion

Tumour margin irregularity and neovascularity are qualitative CT features predictive of microscopic PFI in cT1 RCC undergoing PN. Margin irregularity is the strongest and most reproducible predictor, and a two-feature exploratory nomogram provides a template for future quantitative models. These features represent biologically anchored targets for radiomics-based model development and for the evidence base underpinning structured imaging classification systems such as KI-RADS. Prospective, multicentre studies incorporating quantitative feature analysis and external validation are warranted.

Statements and Declarations

Competing interests The authors have no relevant financial or non-financial interests to disclose.

Data availability The datasets generated and analysed during the current study are not publicly available owing to institutional patient-confidentiality requirements, but de-identified data are available from the corresponding author on reasonable request.

References

1. Capitanio U, Bensalah K, Bex A, Boorjian SA, Bray F, Coleman J et al (2019) Epidemiology of renal cell carcinoma. Eur Urol 75:74–84. https://doi.org/10.1016/j.eururo.2018.08.036

2. Padala SA, Barsouk A, Thandra KC, Saginala K, Mohammed A, Vakiti A et al (2020) Epidemiology of renal cell carcinoma. World J Oncol 11:79–87. https://doi.org/10.14740/wjon1279

3. Laguna MP, Algaba F, Cadeddu J, Clayman R, Gill I, Gueglio G et al (2014) Current patterns of presentation and treatment of renal masses: a clinical research office of the endourological society prospective study. J Endourol 28:861–870. https://doi.org/10.1089/end.2013.0724

4. Gershman B, Thompson RH, Boorjian SA, Lohse CM, Costello BA, Cheville JC et al (2018) Radical versus partial nephrectomy for cT1 renal cell carcinoma. Eur Urol 74:825–832. https://doi.org/10.1016/j.eururo.2018.08.028

5. Sokhi HK, Mok WY, Patel U (2015) Stage T3a renal cell carcinoma: staging accuracy of CT for sinus fat, perinephric fat or renal vein invasion. Br J Radiol 88:20140504. https://doi.org/10.1259/bjr.20140504

6. Ramaswamy K, Kheterpal E, Pham H, Mohan S, Stifelman M, Taneja S et al (2015) Significance of pathologic T3a upstaging in clinical T1 renal masses undergoing nephrectomy. Clin Genitourin Cancer 13:344–349. https://doi.org/10.1016/j.clgc.2015.01.001

7. Gorin MA, Ball MW, Pierorazio PM, Tanagho YS, Bhayani SB, Kaouk JH et al (2013) Outcomes and predictors of clinical T1 to pathological T3a tumor up-staging after robotic partial nephrectomy: a multi-institutional analysis. J Urol 190:1907–1911. https://doi.org/10.1016/j.juro.2013.06.014

8. Nayak JG, Patel P, Saarela O, Liu Z, Kapoor A, Finelli A et al (2016) Pathological upstaging of clinical T1 to pathological T3a renal cell carcinoma: a multi-institutional analysis of short-term outcomes. Urology 94:154–160. https://doi.org/10.1016/j.urology.2016.03.029

9. Veccia A, Falagario U, Martini A, Marchioni M, Antonelli A, Simeone C et al (2021) Upstaging to pT3a in patients undergoing partial or radical nephrectomy for cT1 renal tumors: a systematic review and meta-analysis of outcomes and predictive factors. Eur Urol Focus 7:574–581. https://doi.org/10.1016/j.euf.2020.05.013

10. Shah PH, Moreira DM, Patel VR, Gaunay G, George AK, Alom M et al (2017) Partial nephrectomy is associated with higher risk of relapse compared with radical nephrectomy for clinical stage T1 renal cell carcinoma pathologically up staged to T3a. J Urol 198:289–296. https://doi.org/10.1016/j.juro.2017.03.012

11. Silverman SG, Pedrosa I, Schieda N, Margulis V, Kapur P, Davenport MS (2025) In pursuit of KI-RADS: toward a single, evidence-based imaging classification of renal masses. Radiology 314:e240308. https://doi.org/10.1148/radiol.240308

12. Liu J, Lin Z, Wang K, Fang D, Zhang Y, Wang X et al (2023) A preliminary radiomics model for predicting perirenal fat invasion on renal cell carcinoma with contrast-enhanced CT images. Abdom Radiol (NY) 48:649–658. https://doi.org/10.1007/s00261-022-03699-8

13. Yuan E, Chen Y, Ye L, He B, He C, Ma J et al (2025) Enhanced staging of renal cell carcinoma using tumor morphology features: model development and multi-source validation. NPJ Digit Med 8:305. https://doi.org/10.1038/s41746-025-01723-x

14. Al Mopti A, Alqahtani A, Alshehri AHD, Nabi G (2026) Peritumoral fat radiomics for dual prediction of TNM stage and histological grade in clear cell renal cell carcinoma:

discovery of target-specific optimal imaging distances. Diagnostics (Basel) 16:1099. https://doi.org/10.3390/diagnostics16071099

15. Liu H, Wang Z, Peng E, Chen Z, Tang K, Xia D (2021) Added value of systemic inflammation markers in predicting clinical stage T1 renal cell carcinoma pathologically upstaged to T3a. Front Oncol 11:679536. https://doi.org/10.3389/fonc.2021.679536

16. Ni D, Ma X, Li HZ, Gao Y, Li XT, Zhang Y et al (2018) Factors associated with postoperative renal sinus invasion and perinephric fat invasion in renal cell cancer: treatment planning implications. Oncotarget 9:10091–10099. https://doi.org/10.18632/oncotarget.23497

17. Sun ZH, Huang XJ, Dong JH, Liu Z, Yan Y, Liu C et al (2021) Risk factors of renal sinus invasion in clinical T1 renal cell carcinoma patients undergoing nephrectomy (in Chinese). Beijing Da Xue Xue Bao Yi Xue Ban 53:659–664. https://doi.org/10.19723/j.issn.1671-167X.2021.04.006

18. Renard AS, Nedelcu C, Paisant A, Saulnier P, Le Bigot J, Azzouzi AR et al (2019) Is multidetector CT-scan able to detect T3a renal tumor before surgery? Scand J Urol 53:350–355. https://doi.org/10.1080/21681805.2019.1675756

19. Shimada W, Kimura K, Tanaka H, Fukuda S, Yoshida S, Fujii Y (2022) Significance of tumor shape irregularity: radiomics analysis based on dynamic computed tomography for predicting pT3a upstaging in cT1b-2N0M0 renal cell carcinoma. Int J Urol 29:1387–1389

20. Lee HJ, Kim TM, Park J, Cho JY, Kim SY (2026) Preoperative detection of perirenal fat invasion in renal cell carcinoma: integration of qualitative and quantitative CT parameters. J Comput Assist Tomogr 50:376–382. https://doi.org/10.1097/RCT.0000000000001820

21. Damgaci L, Ozer H, Rona G (2021) Diagnostic value of MDCT in determining the perinephric fat tissue and renal sinus invasion in patients with clear cell renal cell carcinoma. Niger J Clin Pract 24:489–495. https://doi.org/10.4103/njcp.njcp_242_20

22. Landman J, Park JY, Zhao C, Baker M, Hofmann M, Helmy M et al (2017) Preoperative computed tomography assessment for perinephric fat invasion: comparison with pathological staging. J Comput Assist Tomogr 41:702–707. https://doi.org/10.1097/RCT.0000000000000588

23. Guo H, Meng L, Zhu L, Zhang Z, Zhang Y, Sun Z et al (2026) CT-based variables of perirenal fat are risk factors for assessing pathological T-stage in patients with clear cell renal cell carcinoma. Ann Med 58:2625563. https://doi.org/10.1080/07853890.2026.2625563

24. Bradley AJ, MacDonald L, Whiteside S, Johnson RJ, Ramani VA (2015) Accuracy of preoperative CT T staging of renal cell carcinoma: which features predict advanced stage? Clin Radiol 70:822–829. https://doi.org/10.1016/j.crad.2015.03.013

25. Han NY, Sung DJ, Kim MJ, Park BJ, Sim KC, Cho SB (2016) Perirenal fat stranding on CT: is there an association with bladder outlet obstruction? Br J Radiol 89:20160195. https://doi.org/10.1259/bjr.20160195

26. Zhang Z, Yu C, Velet L, Li Y, Jiang L, Zhou F (2016) The difference in prognosis between renal sinus fat and perinephric fat invasion for pT3a renal cell carcinoma: a meta-analysis. PLoS One 11:e0149420. https://doi.org/10.1371/journal.pone.0149420

Figure legends

Fig. 1 Odds ratios for perinephric fat invasion (PFI) from univariable (circles) and multivariable (squares) Firth penalised logistic regression, with profile penalised-likelihood 95% confidence intervals (CI) on a log scale. The multivariable model includes margin irregularity and neovascularity

Fig. 2 Receiver-operating-characteristic curves for prediction of perinephric fat invasion: two-variable model (margin irregularity+neovascularity; solid line) versus margin irregularity alone (dashed line). The dotted diagonal indicates chance. Optimism-corrected area under the curve (AUC) 0.71 and calibration slope 0.98 (1,000 bootstrap resamples). CI, confidence interval

Fig. 3 Exploratory nomogram for microscopic perinephric fat invasion (PFI) derived from the two-variable Firth penalised model (margin irregularity+neovascularity; n=117, 10 events). Apparent area under the curve (AUC) 0.73 (bootstrap 95% confidence interval 0.54–0.90); optimism-corrected AUC 0.71; calibration slope 0.98. Presented for illustration only; not validated for clinical use

Fig. 4 Inter-observer agreement (Fleiss' κ, three readers, n=117) for each CT feature. Filled circles and bars show Fleiss' κ with bootstrap 95% confidence intervals (CI); open circles show pairwise Cohen's κ; shaded bands indicate Landis and Koch agreement categories (substantial, 0.61–0.80; almost perfect, >0.80). CT, computed tomography

Table 1 Baseline characteristics and RENAL nephrometry components of the imaging-analysis cohort (n=117), by perinephric fat invasion status

Variable	No PFI (n=107)	PFI present (n=10)	p-value
Age (y)	58.4±11.1	64.5±10.4	0.10
CT tumour size (cm)	3.09±1.51	3.62±1.54	0.29
RENAL score group			0.195
Low	23 (21.5)	2 (20.0)	
Moderate	38 (35.5)	1 (10.0)	
High	46 (43.0)	7 (70.0)	
Exophytic/endophytic			0.43
1	20 (18.7)	1 (10.0)	
2	63 (58.9)	5 (50.0)	
3	24 (22.4)	4 (40.0)	
Nearness to collecting system			0.622
1	23 (21.5)	1 (10.0)	
2	14 (13.1)	1 (10.0)	
3	70 (65.4)	8 (80.0)	
Location relative to polar lines			0.540
1	29 (27.1)	3 (30.0)	
2	28 (26.2)	4 (40.0)	
3	50 (46.7)	3 (30.0)	

Values are presented as mean±standard deviation or number (%). p-values from the independent t-test (continuous variables) or chi-squared/Fisher's exact test (categorical variables); one p-value is given per categorical variable. CT, computed tomography; PFI, perinephric fat invasion.

Table 2 CT imaging features in the imaging-analysis cohort (n=117), by perinephric fat invasion status

CT feature	No PFI (n=107)	PFI present (n=10)	p-value
Abutting renal contour	101 (94.4)	9 (90.0)	0.575
Tumour margin irregularity	31 (29.0)	7 (70.0)	**<0.01**
Perinephric fat stranding	55 (51.4)	5 (50.0)	0.932
Enhancing nodule in perinephric space	2 (1.9)	2 (20.0)	**<0.01**
Neovascularity in perinephric fat	18 (16.8)	5 (50.0)	**0.012**

Values are presented as number (%). p-values from the chi-squared or Fisher's exact test, as appropriate; bold values indicate $p<0.05$. CT, computed tomography; PFI, perinephric fat invasion.

Table 3 Univariable and multivariable Firth penalised logistic regression for perinephric fat invasion (n=117; 10 events)

Predictor	Univariable OR (95% CI)	p-value	Multivariable OR (95% CI)	p-value
Margin irregularity	5.20 (1.45–22.6)	**0.011**	3.56 (0.78–17.8)	0.101
Neovascularity	4.84 (1.31–18.0)	**0.019**	2.41 (0.55–10.9)	0.242
Fat stranding	0.95 (0.27–3.37)	0.930	–	–
Apparent AUC (95% CI)			0.73 (0.54–0.90)	
Optimism-corrected AUC			0.71	
Calibration slope			0.98	

Odds ratios with profile penalised-likelihood 95% CI; p-values from penalised likelihood-ratio tests; bold values indicate $p<0.05$. The multivariable model includes margin irregularity and neovascularity. Fat stranding was pre-specified but showed no univariable association and was not carried forward. Apparent AUC with percentile bootstrap 95% CI; optimism-corrected AUC and calibration slope from bootstrap internal validation. AUC, area under the receiver-operating-characteristic curve; CI, confidence interval; OR, odds ratio.

Table 4 Inter-observer agreement (three readers) and diagnostic performance (primary reader) of each CT feature for perinephric fat invasion (n=117)

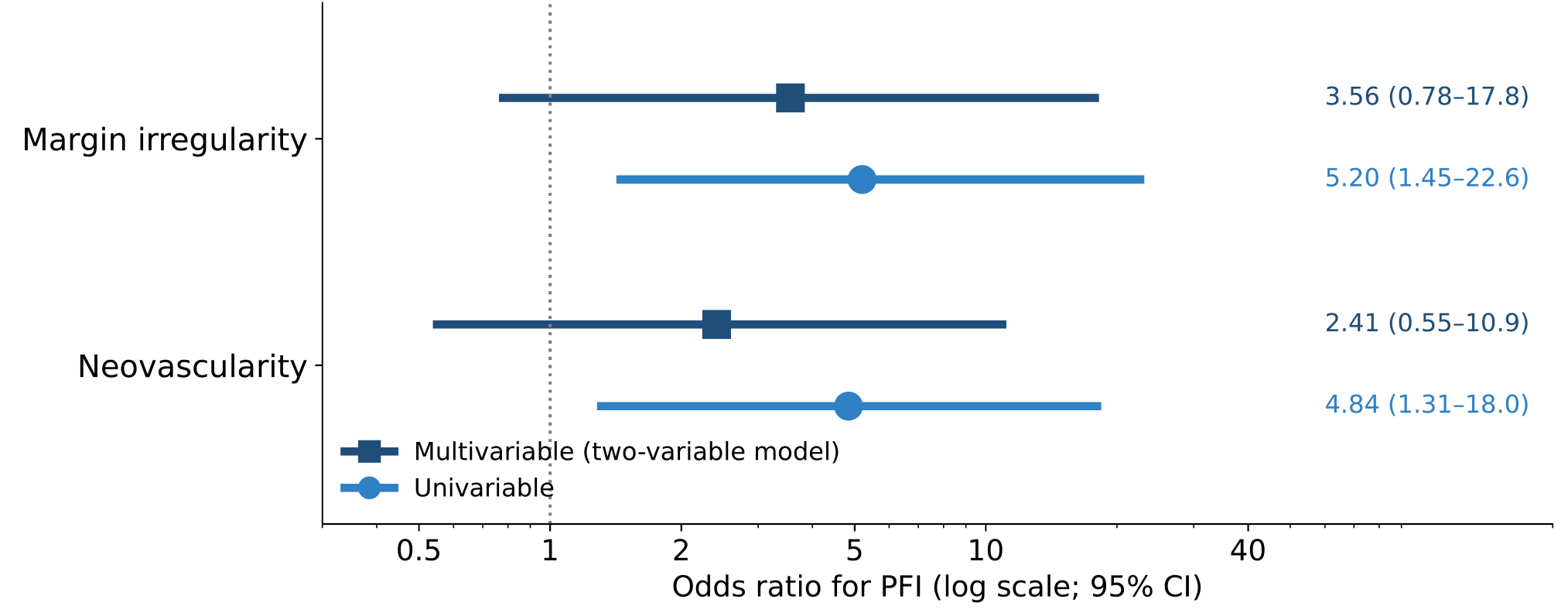
Feature	Fleiss' κ (95% CI)	Cohen's κ R1 vs. R2	Cohen's κ R1 vs. R3	Cohen's κ R2 vs. R3	Sensitivity	Specificity	PPV	NPV
Margin irregularity	0.67 (0.55–0.77)	0.65 (0.50–0.79)	0.56 (0.40–0.71)	0.79 (0.67–0.90)	0.70	0.71	0.18	0.96
Neovascularity	0.74 (0.60–0.85)	0.76 (0.59–0.89)	0.71 (0.56–0.86)	0.74 (0.58–0.88)	0.50	0.83	0.22	0.95
Fat stranding	0.68 (0.57–0.78)	0.73 (0.61–0.85)	0.59 (0.44–0.73)	0.72 (0.59–0.84)	0.50	0.49	0.08	0.91
Enhancing nodule	0.65 (0.19–0.92)	0.85 (0.00–1.00)	0.65 (−0.01–1.00)	0.48 (−0.02–0.88)	0.20	0.98	0.50	0.93
Contour abutment	0.83 (0.63–0.96)	0.81 (0.53–1.00)	0.79 (0.47–1.00)	0.88 (0.65–1.00)	–	–	–	–

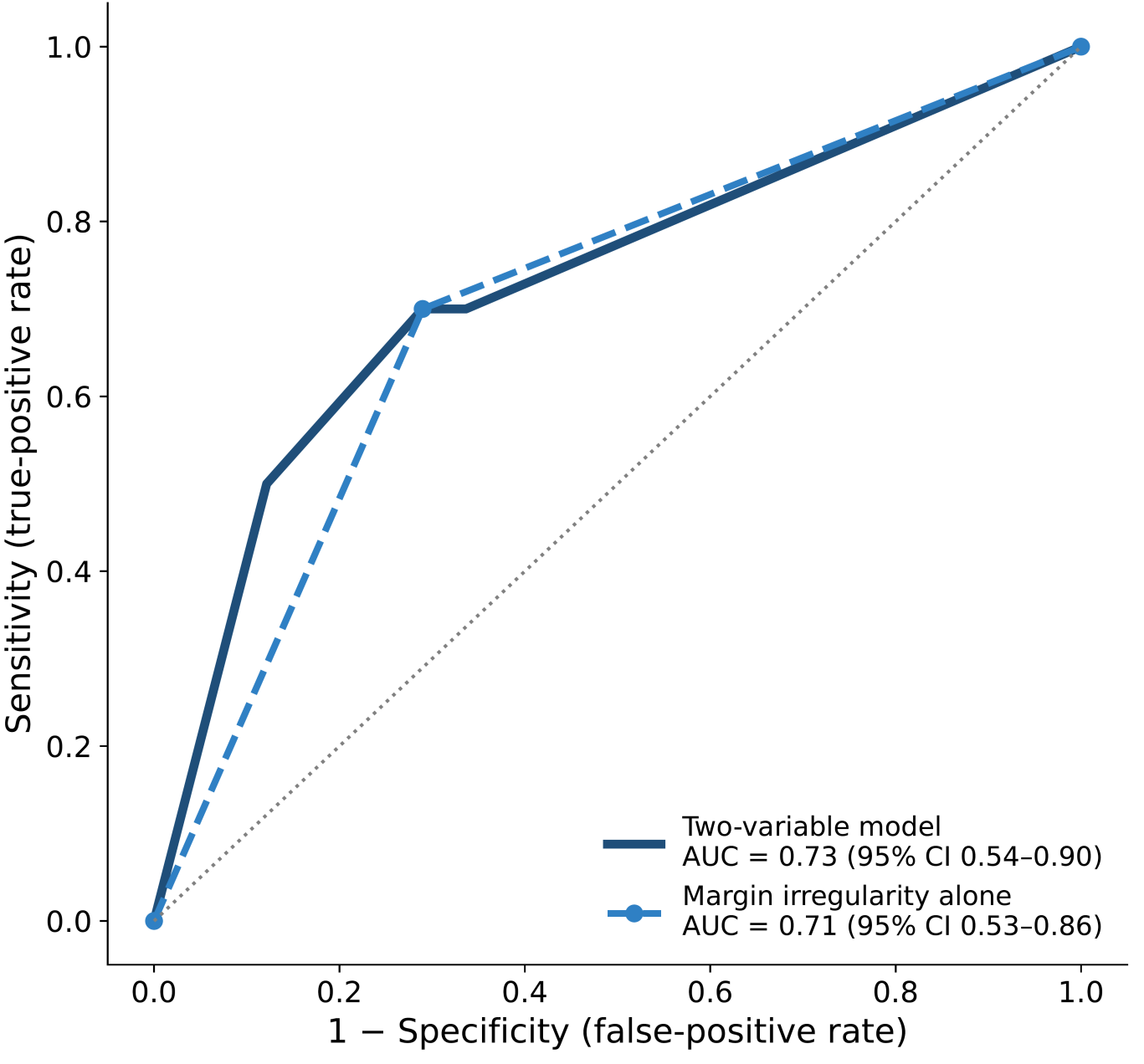
κ values with percentile bootstrap 95% CI (2,000 resamples). R1, primary uroradiologist, whose scores were used for all association, modelling and diagnostic performance analyses; R2 and R3, reproducibility readers. Confidence intervals for enhancing nodule are wide because the feature was present in few patients. CI, confidence interval; CT, computed tomography; NPV, negative predictive value; PPV, positive predictive value.

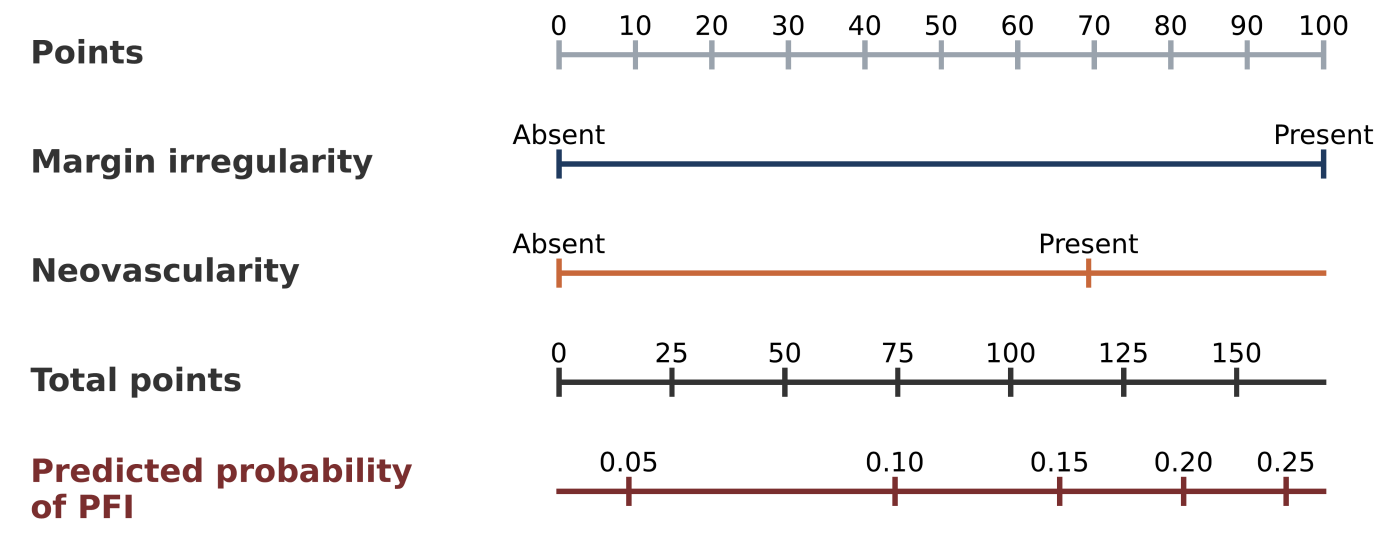
Table 5 Observed and predicted probability of perinephric fat invasion by feature combination (two-variable model, n=117)

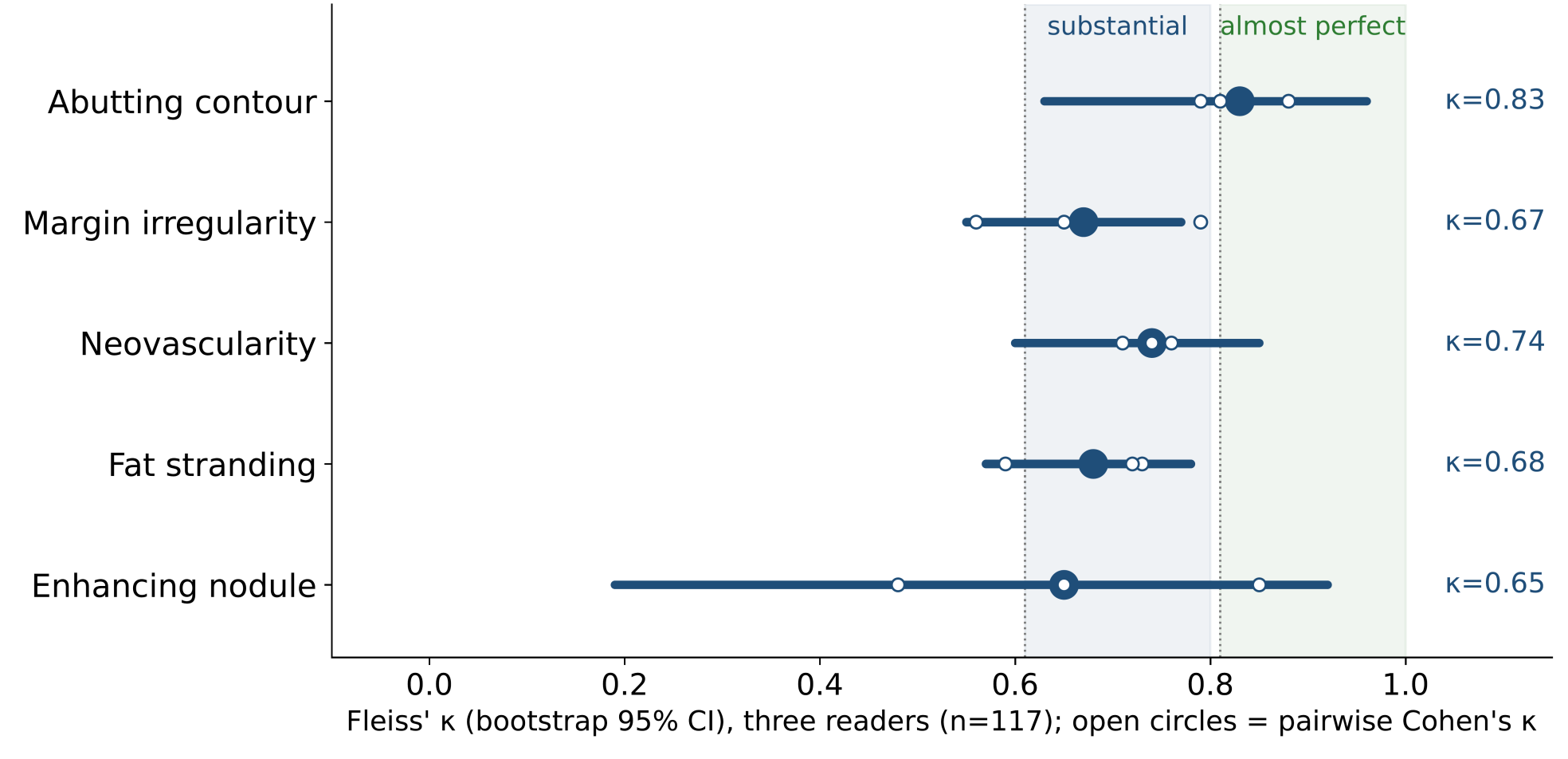
Margin irregularity	Neovascularity	Patients	PFI	Observed PFI (%)	Predicted PFI (%)
Absent	Absent	74 (63)	3	4.1	4.1
Absent	Present	5 (4)	0	0	9.4
Present	Absent	20 (17)	2	10.0	13.3
Present	Present	18 (15)	5	27.8	27.0

Values are presented as number (%) or number only. Predicted probabilities from the two-variable Firth penalised logistic regression model. PFI, perinephric fat invasion.


Margin irregularity
Neovascularity
3.56 (0.78–17.8)
5.20 (1.45–22.6)
2.41 (0.55–10.9)
4.84 (1.31–18.0)
Multivariable (two-variable model)
Univariable
0.5
1
2
5
10
40
Odds ratio for PFI (log scale; 95% CI)


1.0
0.8
0.6
0.4
0.2
0.0
Sensitivity (true-positive rate)
0.0
0.2
0.4
0.6
0.8
1.0
1 − Specificity (false-positive rate)
Two-variable model
AUC = 0.73 (95% CI 0.54–0.90)
Margin irregularity alone
AUC = 0.71 (95% CI 0.53–0.86)


Points
0
10
20
30
40
50
60
70
80
90
100
Margin irregularity
Absent
Present
Neovascularity
Absent
Present
Total points
0
25
50
75
100
125
150
Predicted probability of PFI
0.05
0.10
0.15
0.20
0.25


substantial
almost perfect
Abutting contour
Margin irregularity
Neovascularity
Fat stranding
Enhancing nodule
κ=0.83
κ=0.67
κ=0.74
κ=0.68
κ=0.65
0.0
0.2
0.4
0.6
0.8
1.0
Fleiss' κ (bootstrap 95% CI), three readers (n=117); open circles = pairwise Cohen's κ